Ultraviolet multi-spectral microscopy using iterative phase-recovery from chromatic aberrations

Ojaghi, Ashkan, Robles, Francisco

Ashkan Ojaghi, Francisco E. Robles, "Ultraviolet multi-spectral microscopy using iterative phase-recovery from chromatic aberrations," Proc. SPIE 10887, Quantitative Phase Imaging V, 108870M (4 March 2019); doi: 10.1117/12.2508972

SPIE.

Event: SPIE BiOS, 2019, San Francisco, California, United States

Ultraviolet multi-spectral microscopy using iterative phase-recovery from chromatic aberrations

Ashkan Ojaghi[a], Francisco E. Robles*[a]
[a]Wallace H. Coulter Dept. of Biomedical Engineering, Georgia Institute of Technology and Emory University, 313 Ferst Dr. NW, Atlanta, GA 30332, USA

ABSTRACT

The ultraviolet region of the spectrum offers unique capabilities for label-free molecular imaging of biological samples by providing highly-specific, quantitative information of many important endogenous biomolecules. However, the application of UV spectral imaging to biomedicine has been limited. To this end, we have recently introduced ultraviolet hyperspectral interferometric (UHI) microscopy, which applies interferometry to overcome significant challenges associated with UV spectroscopy when applied to molecular imaging.

Here we present an alternative approach for UV multi-spectral microscopy which enables faster wide-field imaging at the expense of fewer spectral data points. Instead of line-scanning to recover high-resolution spectral information with an imaging spectrometer, we detect a wide field-of-view using a UV-sensitive camera and recover the spectral information using several (>5) UV-filters. Moreover, rather than using interferometry to recover the phase to correct for chromatic aberrations, we leverage the chromatic aberrations themselves to obtain a stack of through-focus intensity images (at various wavelengths) and then apply an iterative solution of the Transport of Intensity (TIE) equation to recover the phase and produce in-focus images at all wavelengths without moving the sample or objective. This configuration greatly simplifies the instrumentation, reducing its footprint and making it less expensive, while enabling fast, wide area imaging with better photon efficiency. We assess the capabilities of this technique through a series of simulations and experiments on red blood cells, which show good quantitative agreement with UHI and tabulated hemoglobin absorption properties. Potential biomedical applications are also discussed.

Keywords: Ultraviolet microscopy, Phase recovery, Transport of intensity equation, Digital refocusing, Molecular imaging, Red blood cells

1. INTRODUCTION

Deep-ultraviolet microscopy is a powerful technique that enables assessment of biochemical and structural properties of biological samples. This method offers many advantages over conventional microscopy techniques such as higher spatial resolution due to the light's shorter wavelength. Deep-UV microscopy also yields access to many endogenous biomolecules that play an important role in cell function and structure because they possess unique absorptive and dispersive features in this spectral range (e.g., 250-450nm)[1-2]. In addition, the UV microscopy images carry quantitative information about the biochemical components of samples which can be extracted as mass maps[3-4].

Unfortunately, application of deep-UV microscopy has been limited due to a number of challenges such as less than optimal cameras and light sources, phototoxicity, strong fluorescent background, and severe chromatic aberration[4]. However, recent technological advancements in high-quantum efficiency UV cameras and broadband light sources have enabled progress to address some of these limitations and have thus led to the development of UV microscopy techniques to study biological samples. For example, Zeskind et al. demonstrated continuous imaging of live cells using deep-UV light for over 6 hours before inducing irreversible cell damage[3]. Recently, a novel method named ultraviolet hyperspectral interferometric (UHI) microcopy has been demonstrated which leverages these recent advances along with coherent detection to overcome all of the aforementioned limitations of microscopy in the deep-UV region of the spectrum[4]. UHI microscopy uses a 4f interferometric configuration that allows coherent detection using an incoherent, broadband light source[4]. The setup consists of a modified Mach-Zehnder interferometer which provides access to the complex optical fields across a deep-UV range (240-450 nm), making it possible to extract quantitative spectroscopic information of both the

* francisco.robles@bme.gatech.edu

Quantitative Phase Imaging V, edited by Gabriel Popescu, YongKeun Park, Proc. of SPIE Vol. 10887, 108870M

absorptive and dispersive properties of many endogenous biomolecules. The complex field information carries quantitative phase information from sample and allows us to correct for the chromatic aberration in the system using digital refocusing techniques.

In this study, we present a non-interferometric configuration to enhance the throughput and photon efficiency of deep-UV microscopy system, enabling fast wide-field imaging at the expense of fewer spectral data points. In this configuration, we use a UV-sensitive CCD camera to image a wide field-of-view instead of the line-scanning to recover high-resolution spectral information with an imaging spectrometer in UHI microscopy. Moreover, rather than using interferometry to recover the phase to correct for chromatic aberrations, we leverage the chromatic aberrations focal length shift of our UV objective to obtain a stack of through-focus intensity images at various wavelengths. Using an iterative solution of the Transport of Intensity (TIE) equation we recover the phase and produce an in-focus multi-spectral image stack without moving the sample or objective. We assess the capabilities of this technique through a series of simulations and experiments on a standard phase target as well as live red blood cells.

2. EXPERIMENTAL SETUP AND METHODS

2.1 Experimental setup

The developed deep-UV multi-spectral microscopy system consists of an incoherent broadband laser-driven plasma light source (EQ-99X LDLS, Energetiq Technology). The output light from the broadband source is collimated through a set of off-axis parabolic mirrors (Newport Corporation) and relayed to the sample using a 300mm lens. Multi-spectral imaging is done using UV bandpass filters installed on a filter wheel, allowing acquisition of images at six wavelength regions at 255, 280, 300, 340, and 380nm. For imaging, we use 40X (NA 0.5) (LMU-40X, Thorlabs), UV microscope objectives and achieve an average spatial resolution of ~300 nm. Images are then recorded using a UV sensitive CCD camera (integration time is set at 30-100ms range) while sample is translated and adjusted for focusing via a three-axis high-precision motorized stage (MLS2031, Thorlabs).

2.2 Digital refocusing using angular spectrum method

The out-of-focus amplitude images are refocused to mitigate the effects of chromatic aberration in the UV range using an angular spectrum transformation method. In this method, the complex field, which is composed of the measured amplitude and phase of light, is refocused at all wavelengths using a Fresnel transformation[5], where the wavefronts are digitally propagated. Based on the schematic depicted in Fig.1c, the angular spectrum of the light field is calculated using a 2D Fourier transform and digitally propagated using the free space propagation transfer function calculated according to the chromatic aberration-induced focal length shift of the UV objective (see Fig. 1a). The amplitude and phase of the propagated field is then recovered by applying an inverse Fourier transform on the angular spectrum. This process yields focused amplitude and phase images (example shown in Fig. 1b) throughout the imaging spectral range (e.g., 255-415nm).

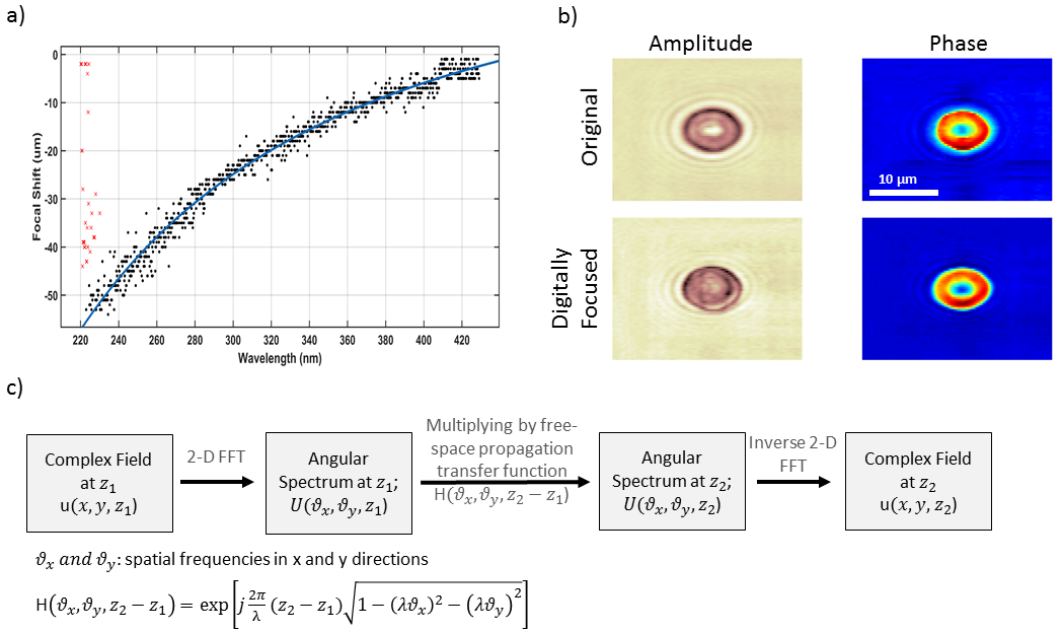

Figure 1. a) Chromatic aberration-induced focal length shift of the UV objective (adapted from ref. 4) b) Amplitude and phase images of a red blood cell before and after digital refocusing (adapted from ref. 4) c) Angular spectrum method for free space field propagation

2.3 Standard Phase target sample

In order to test the capabilities of our system we manufactured a quartz phase target. Patterns with different thicknesses are etched on quartz slides to provide various phase delays to the light field at passes through the medium. The phase target is then imaged at the focal plane of the objective at 300 nm (in focus sample plane) and at other wavelengths (i.e., 255, 280, 340, and 380nm) using the deep-UV microscopy system to obtain the though-focus image stack.

2.4 Red blood sample preparation

Whole blood is collected from healthy donors and added to an anticoagulant solution (sodium citrate, Beckton Dickenson) according to approved protocols by Institutional Review Board of Georgia Institute of Technology. Live red blood cells (RBCs) are then isolated by centrifuging the whole blood sample at 150 g for 10 minutes and resuspending in Phosphate-buffered saline (PBS) (Calbiochem). The cell suspension is pipetted into an imaging chamber placed on a quartz microscope slide and sealed with a quartz coverslip to avoid contamination and evaporation during the experiments.

3. ITERATIVE PHASE RECOVERY FROM CHROMATIC ABBERATION

The developed UV microscopy setup enables us to obtain images of biological samples at different wavelengths in the deep-UV range (i.e., 255, 280, 300, 340, and 380nm). Due to presence of chromatic aberrations in our system, the effective focal length of microscope objective changes as a function of wavelength of light used for microscopy. Accordingly, we can obtain an in-focus image by placing the sample at the focal plane of the UV objective at a certain wavelength while images obtained at any other wavelength will appear defocused, forming a through-focus image stack. Having access to quantitative phase information of the sample, we can refocus the out-of-focus amplitude images using digital refocusing technique described in section 2.2 to obtain an in-focus multi-spectral image stack. However, in a non-interferometric configuration we no longer have access to phase information from sample. To overcome this limitation, we employ a phase-recovery technique based on an iterative solution of the Transport of Intensity (TIE) equation. This equation is derived based on the paraxial wave equation after defocus and is described by Fresnel propagation[6]:

$$\frac{\partial I(x,y)}{\partial \xi} = \frac{-\overline{\nabla}\perp\cdot[I(x,y)\nabla\varphi(x,y)]}{2\pi} \quad (1)$$

where $I(x, y)$ is the intensity, $\varphi(x, y)$ is the phase, and $\nabla\perp$ is the two-dimensional gradient operator in the lateral dimensions. In this equation, wavelength λ and distance z are interchangeable while their product describes the chromatic

defocus ($\xi = \lambda z$). Solving this equation enables phase recovery using images obtained at different wavelengths in a single plane of constant z. One approach for recovering phase through TIE equation is to find an estimate of the phase and refining the initial phase estimate via free space propagation of the estimated complex field between the image planes corresponding to different defocus images. By updating the amplitude of the complex field using the measured amplitude images we can approach the correct phase estimate after several iterations. In this algorithm, we take into account the differences between the dispersive and absorptive properties of the sample at different wavelengths by scaling our amplitude and phase estimate accordingly. For example, to propagate from 300nm plane to 280nm we scale the amplitude using the ratio of the absorption coefficient of the two wavelengths ($I_{280nm} = exp\,[\log(I_{300nm})(\mu_{a\,@\,280nm}/\mu_{a\,@\,300nm})]$) and use the refractive indices to scale phase ($\varphi_{est\,@\,280nm} = \varphi_{est\,@\,300nm}\,[K_{280nm}n_{@\,280nm}/K_{300nm}n_{@\,300nm}]$). After scaling, we form the estimated complex field for the in-focus sample plane by assuming a constant phase profile and use the angular spectrum free space propagation approach to each out-of-focus sample plane where we keep the phase and update the amplitude and propagate the complex field back to the in-focus plane. By repeating this approach for all the though-focus image stack over several iterations we obtain the phase estimate which then is used to propagate the out-of-focus images to obtain the in-focus multi-spectral image stack.

4. RESULTS AND DISCUSSION

4.1 Phase recovery based on simulation of a red blood cell

To evaluate the efficacy of our iterative phase recovery algorithm we simulate a though-focus image stack using a red blood cell model and according to the absorptive and dispersive properties of these cells. Figure 2a shows the thickness profile used for simulation of the amplitude and phase images at the in-focus image plane based on the absorption coefficients and refractive indices of a human red blood cell reported in ref 4. We assume that the in-focus image is captured at 300nm wavelength (Fig. 2b and 2c) while the defocus images are obtained at 255, 280, 340, 380nm. Using the simulated phase and amplitude at 300nm and the free-space propagation scheme we can obtain the though-focus image stack shown in Fig. 2c.

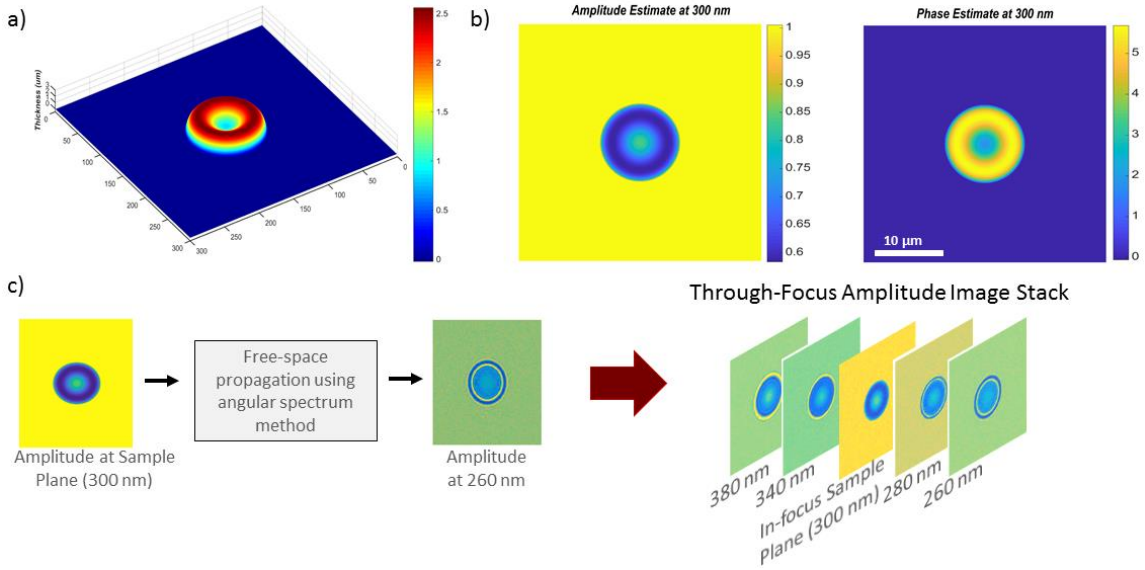

Figure 2. a) Thickness profile of a red blood cell used for simulations b) Amplitude and phase estimate for a red blood cell at 300nm wavelength c) Simulation of a through-focus image stack based on the in-focus complex field and free-space propagation

By applying the iterative phase recovery algorithm described in section 3 we estimate the phase profile and use it for propagation of the out-of-focus images to the in-focus image plane. The resulting phase estimate is depicted in Fig.3a and 3b, showing a good agreement with the simulated phase profile. Further, the amplitude profiles extracted from out-of-focus images along with the refocused images using both the simulated and recovered phase are shown in Fig. 3c for different wavelengths. The amplitude profiles demonstrate the effect of digital refocusing and show a good agreement between profiles obtained from refocusing using simulated (expected) and recovered (estimated) phase images. The effect

of refocusing and the agreement between results can also be verified in amplitude images depicted in Fig. 3d. The results from RBC simulation show the efficacy of our iterative algorithm for phase recovery using through-focus image stack based on a prior knowledge of absorptive and dispersive properties of the sample.

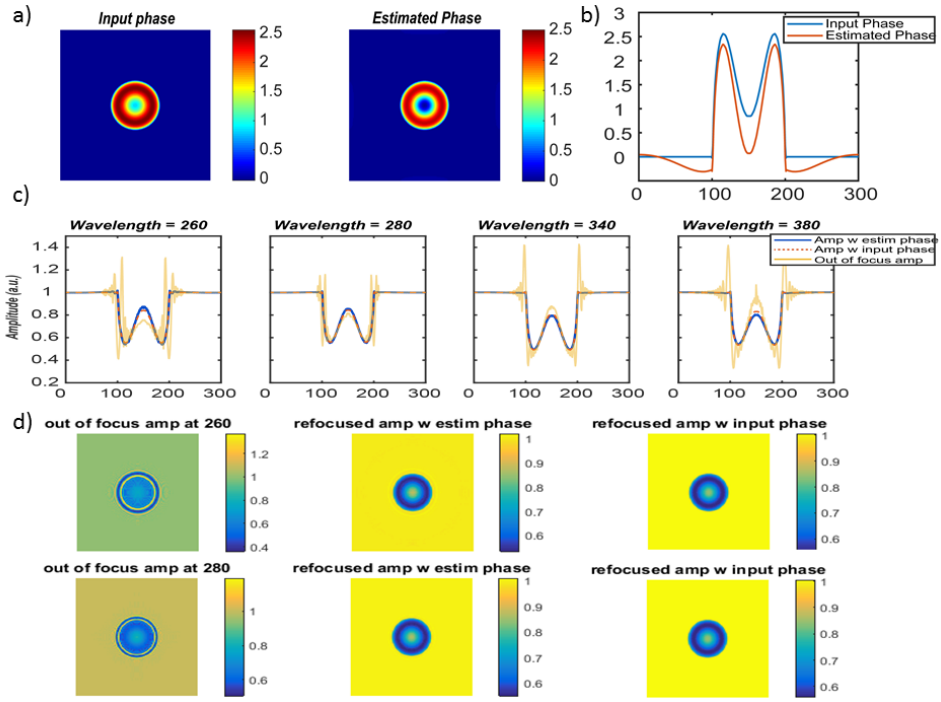

Figure 3. a) Simulated phase profile and the estimated phase from iterative recovery algorithm b) Phase profile plotted over a line going through the center of image c) Amplitude profiles from out-of-focus images, refocused images using the simulated and recovered phase profiles d) out-of-focus amplitude images at 260 and 280nm wavelengths along with the refocused images using the recovered (estimated) and simulated (input) phase profiles

4.2 Multi-spectral imaging and phase recovery for a standard phase target

As the next step, we apply our iterative phase recovery technique to though-focus image stack obtained from a sample with known optical properties. To this end, we manufactured a standard phase target according to section 2.3 and performed multi-spectral imaging on a 200nm thick pattern (shown in Fig. 4a) to obtain a through-focus image stack. Then, we apply the iterative phase recovery algorithm on the data to estimate the phase profile at the in-focus sample plane (at 300nm wavelength). By dividing the estimated phase by the refractive index of quartz at 300 nm wavelength we calculate the sample thickness profile, shown in Fig. 4b. The thickness distribution are close to the actual pattern height (i.e., 200nm) which verifies the accuracy of the phase estimation. Lastly, using our phase estimate we back-propagate the out-of-focus amplitude images to form the in-focus image stack depicted in Fig. 4c.

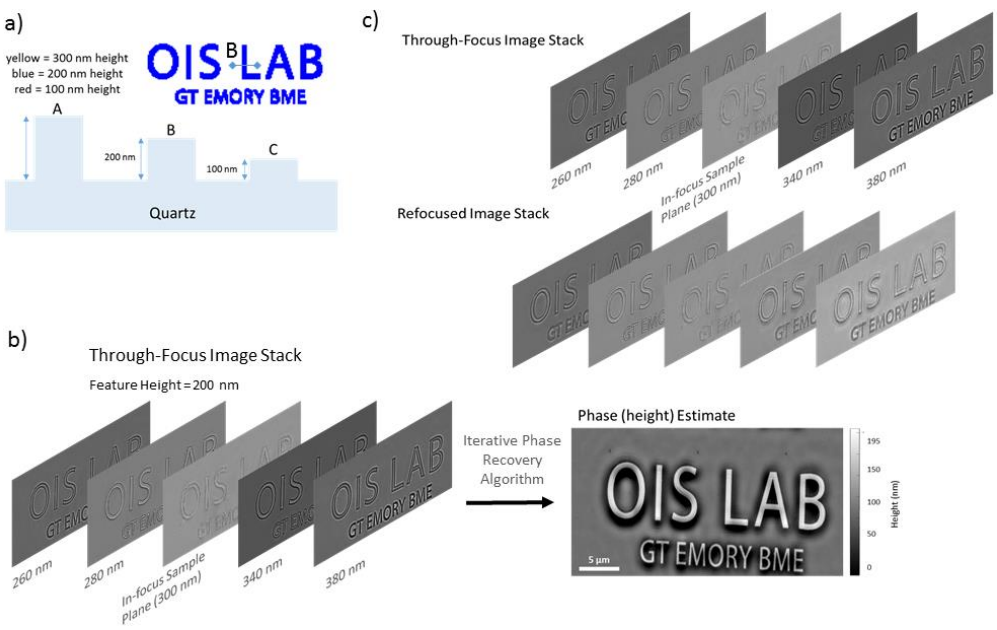

Figure 4. a) Schematic of the manufactured standard phase target on a quartz slab b) Height profile obtained from a through-focus image stack from a pattern with 200nm height c) In-focus image stack obtained by refocusing the though-focus stack via recovered phase profile

4.3 Multi-spectral imaging and phase recovery for live red blood cells

As the final step, we apply our method on images obtained from live human red blood cells in the deep-UV range. In this case, we only use the dispersion properties of water as a generic material to perform phase scaling. By estimating the phase profile and refocusing the images we can obtain the in-focus multi-spectral image stack from the sample which is shown in Fig. 5. To validate our results, we performed the digital refocusing on the through-focus image stack based on the quantitative phase profiles of the cells measured using ultraviolet hyperspectral interferometric microscopy technique (details available in ref. 4). The results from both methods are shown in Fig. 5, demonstrating a good agreement between the resulting in-focus amplitude images.

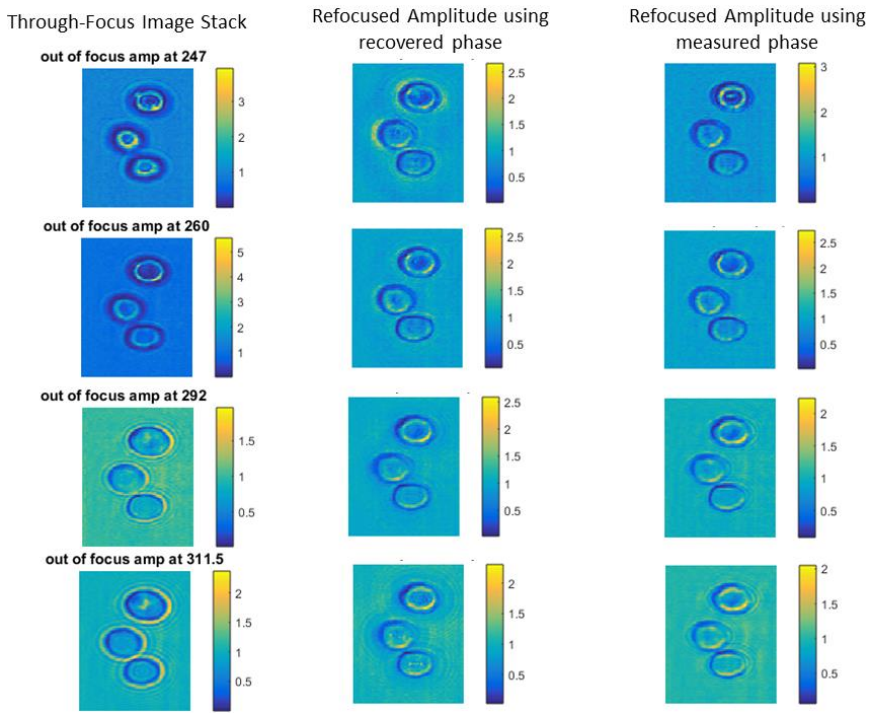

Figure 5. Through-focus images stack along with the refocused images using recovered and measured phase profiles

Having access to the amplitude images, we now can extract quantitative absorption properties of cellular hemoglobin by averaging the optical density within cells ($OD(\lambda) = \mu_{Hb}(\lambda) \cdot t$) and calculating the average molar extinction coefficient ($\varepsilon_{Hb}(\lambda) = \mu_{Hb}(\lambda)/c_{Hb}$). Here, we use an average thickness for a healthy red blood cell $t = 2\,\mu m$ and a typical hemoglobin concentration of $c_{Hb} = 30\ g/dL$[7]. As shown in Fig. 6 the resulting molar extinction coefficient are in agreement with extracted values from images refocused using the measured phase as well as the previously published hemoglobin absorption data[8].

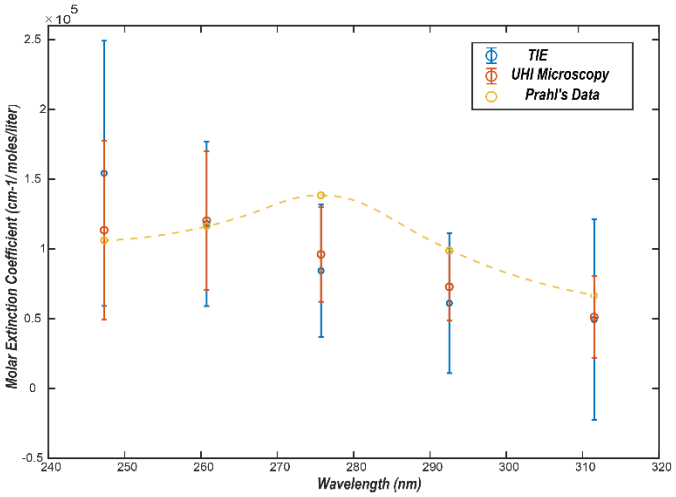

Figure 6. Molar extinction coefficient from hemoglobin within live human red blood cells obtained from refocused images using recovered (TIE) and measured (UHI microscopy) plotted against tabulated hemoglobin data from ref. 8

5. CONCLUSION

In this study, we present a novel ultraviolet multi-spectral microscopy method for label-free molecular imaging of live cells based on an iterative phase-recovery algorithm and digital refocusing. Our approach enables spatial multiplexing via a non-interferometric system design for phase-sensitive microscopy in the deep-UV spectral region. We verify the phase recovery method using simulation of red blood cells as well as experimental results from a standard phase target. Furthermore, we demonstrate that this method offers quantitative endogenous molecular information from live human red blood cells which are validated using UV hyperspectral interferometric microscopy and tabulated hemoglobin absorption data.

ACKNOWLEDGEMENTS

We greatly acknowledge support for this work by the National Science Foundation (NSF CBET CAREER 1752011), Burroughs Welcome Fund (CASI BWF1014540), Galloway Foundation, and Integrated Cancer Research Center at Georgia Institute of Technology.

REFERENCES

[1] Soltani, S., Ojaghi, A., and Robles, F. E., "Deep UV dispersion and absorption spectroscopy of biomolecules," Biomed. Opt. Exp. 10(2), 487-499 (2019).
[2] Katz, A. and Alfano, R., "Optical biopsy-detecting cancer with light," Biomed. Opt. Spectrosc. (1996).
[3] Zeskind, B. J., Jordan, C. D., Timp, W., Trapani, L., Waller, G., Horodincu, V., ... and Matsudaira, P., "Nucleic acid and protein mass mapping by live-cell deep-ultraviolet microscopy," Nat. Methods 4(7), 567 (2007).
[4] Ojaghi, A., Fay, M. E., Lam, W. A., and Robles, F. E., "Ultraviolet Hyperspectral Interferometric Microscopy," Sci. rep. 8(1), 9913 (2018).
[5] Goodman, J. W., [Introduction to Fourier Optics, McGraw-Hill], San Francisco, New York (2005).
[6] Waller, L., Kou, S. S., Sheppard, C. J., and Barbastathis, G., "Phase from chromatic aberrations," Opt. exp. 18(22), 22817-22825 (2010).
[7] Robles, F. E., and Wax, A., "Separating the scattering and absorption coefficients using the real and imaginary parts of the refractive index with low-coherence interferometry," Opt. let. 35(17), 2843-2845 (2010).
[8] Prahl, S., "Optical absorption of hemoglobin," http//omlc. ogi. edu/spectra/hemoglobin (1999).